

The light curve of the companion to PSR B1957+20

M.T. Reynolds^{1*}, P.J. Callanan¹, A.S. Fruchter², M.A.P. Torres³
M.E. Beer⁴ and R.A. Gibbons⁵

¹*Physics Department, University College Cork, Ireland*

²*Space Telescope Science Institute, 3700 San Martin Drive, Baltimore, MD 21218, USA*

³*Harvard-Smithsonian Center for Astrophysics, 60 Garden Street, Cambridge, MA 02138, USA*

⁴*Department of Physics and Astronomy, University of Leicester, Leicester LE1 7RH, England*

⁵*Department of Physics and Astronomy, Vanderbilt University, P.O. Box 1807, Nashville, TN 37240, USA*

22 November 2018

ABSTRACT

We present a new analysis of the light curve for the secondary star in the eclipsing binary millisecond pulsar system PSR B1957+20. Combining previous data and new data points at minimum from the Hubble Space Telescope, we have 100% coverage in the R-band. We also have a number of new K_s -band data points, which we use to constrain the infrared magnitude of the system. We model this with the Eclipsing Light Curve code (ELC). From the modelling with the ELC code we obtain colour information about the secondary at minimum light in BVRI and K. For our best fit model we are able to constrain the system inclination to $65^\circ \pm 2^\circ$ for pulsar masses ranging from $1.3 - 1.9 M_\odot$. The pulsar mass is unconstrained. We also find that the secondary star is not filling its Roche lobe. The temperature of the un-irradiated side of the companion is in agreement with previous estimates and we find that the observed temperature gradient across the secondary star is physically sustainable.

Key words: binaries: eclipsing – pulsars: individual (PSR B1957+20) – stars: neutron, low mass

1 INTRODUCTION

The binary millisecond pulsar (MSP) PSR B1957+20 (Fruchter, Stinebring & Taylor 1988) is the original and one of the best studied members of its class. It consists of a 1.6 ms radio pulsar orbiting a companion of mass no less than $0.022 M_\odot$, in a binary of orbital period 9.17 hours. For 10% of this orbit, the radio emission from the pulsar is eclipsed: the eclipsing region is considerably larger than the Roche lobe of the companion star, suggesting a wind of material from the secondary star, due to ablation by the impinging pulsar radiation (Fruchter et al. 1988). The optical counterpart to PSR B1957+20 was discovered by Kulkarni, Djorgovski & Fruchter (1988); subsequent observations by Callanan, van Paradijs & Rengelink (1995) found the optical counterpart to vary by a factor of 30–40 in flux over the course of the orbital period. These observations are hampered by the close proximity of a line of sight “contaminator”, only $\sim 0.7''$ away.

At the time of its discovery it was assumed that PSR B1957+20 was the missing link between low-mass X-ray binaries (LMXBs) and isolated millisecond pulsars. It was suggested that the high energy pulsar radiation could evaporate the companion star (Ruderman et al. 1989a & 1989b) leaving behind an isolated millisecond pulsar like PSR B1937+21 (Backer et al. 1982).

However, the means by which such a scenario could occur is still the subject of debate (Eichler & Levinson 1988 & 1991; see also Bhattacharya & van den Heuvel 1991, Phinney & Kulkarni 1994 and Lorimer 2001 for thorough reviews of the formation and evolution of MSPs, binary MSPs and the current status of MSP research respectively).

PSR B1957+20 is a member of a class of binary pulsar systems, the Black Widow Pulsars (e.g. King, Davies & Beer 2003). These are systems with secondaries of mass typically less than $0.05 M_\odot$ and orbital period less than 10 hours. To date 15 such systems have been identified¹, with 13 of these residing in globular clusters and only 2 situated in the field. Radio eclipses have been detected in approximately half of the cluster systems and in both of the field systems. Optical light curves exist for only the field systems, PSR B1957+20 (Callanan et al. 1995) and PSR J2051-0827 (Stappers et al. 1999, 2001).

Previous attempts at modelling the optical light curve of PSR B1957+20 had one major limitation: the companion was undetectable at minimum. As such it was impossible to tightly constrain important system parameters such as the inclination or the degree of Roche lobe filling. However, a number of R & I-band images of the optical counterpart at minimum were subsequently obtained

* email : m.reynolds@ucc.ie

¹ <http://www.atnf.csiro.au/research/pulsar/psrcat/expert.html>, Manchester et al. (2005)

by the Hubble Space Telescope (HST). Furthermore, we have recently acquired a number of K_s -band images of the near infrared counterpart. In this paper we combine these data for the first time to model the light curve to obtain tight constraints on the inclination and Roche lobe filling fraction.

2 DATA

2.1 Optical Photometry

The data set consists of B, V and R-band images taken with the William Herschel Telescope (WHT) at La Palma on the nights of 1989 July 2-5 (see Callanan et al. 1995 and references therein for details of the observations), along with two pairs of R (1994 Aug 30, Oct 28) & I-band (1994 Sep 03, Oct 27) data points taken at minimum with the HST.

We re-reduced the WHT data using the IRAF² implementation of DAOPHOT (Stetson 1987). We undertook this task as, in their original analysis, Callanan et al. (1995) used only approximately half of their data due to poor seeing during 2 of the 4 nights of their observing run. Our re-analysis allows us to use an additional night of data. In the end we had 41 useful R-band data-points covering $\sim 85\%$ of the orbit, 39 V-band data points covering $\sim 70\%$ of orbital phase and 7 useful B-band points taken near maximum.

Two R-band & 2 I-band data points were also obtained during eclipse with the Wide Field Planetary Camera 2 using the F675W and F814W filters respectively. The exposure time was 600s in each case. These images were corrected for cosmic ray hits and the object magnitudes were calculated using the QPHOT task in IRAF. The F675W and F814W magnitudes were converted to R and I-band magnitudes in the Johnson system following the prescription given by Holtzman et al. (1995).

The WHT and HST data was then phased according to the radio ephemerides of Ryba & Taylor (1991) and Arzoumanian et al. (1994) respectively. When combined, these points provide the first complete optical light curve of PSR B1957+20, in addition to colour information throughout the orbital cycle.

2.2 IR photometry

Our observations consist of a series of K_s -band images obtained with the 6.5m Magellan Baade telescope at Las Campanas Observatory on 2004 July 23 and 2005 September 13 using the PANIC camera. These were dark-current subtracted, flat fielded, background subtracted and combined using standard IRAF routines. In total we obtained 4 images totalling approximately 18 minutes on source exposure time. We display one of our K_s -band ($1.99\mu\text{m} \leq \lambda \leq 2.30\mu\text{m}$) images in Fig. 1. The companion star to the pulsar is easily resolved.

Photometry was carried out in the same manner as the WHT optical data. The image was calibrated using the standard star P565-C (Persson et al. 1998) and cross checked by comparing a number of stars in our field with those in the 2MASS catalogue. The data was phased using the ephemeris of Arzoumanian et al. (1994),

Table 1. K_s magnitudes of PSR B1957+20.

ϕ	Secondary K_s mag	Contaminator K_s mag
0.5	17.8 ± 0.1	18.06 ± 0.06
0.764	18.20 ± 0.05	17.98 ± 0.04
0.774	18.27 ± 0.10	18.13 ± 0.08
0.788	18.35 ± 0.06	18.02 ± 0.05
0.824	18.73 ± 0.09	18.11 ± 0.07

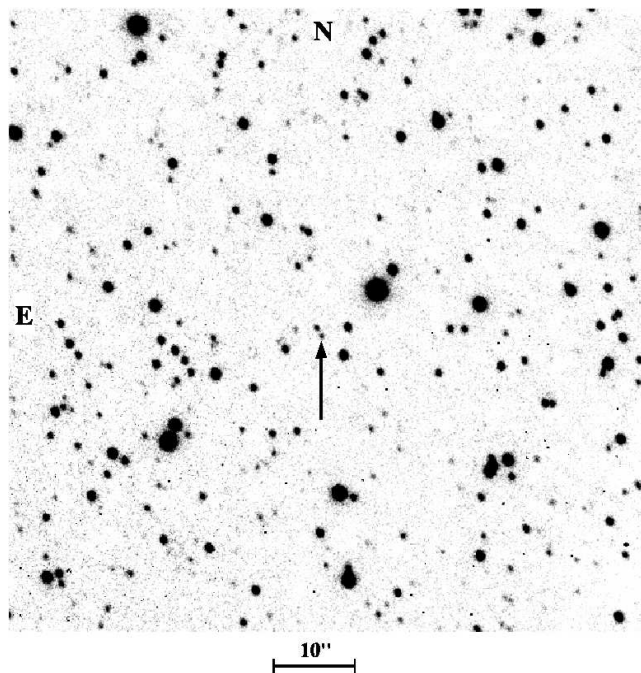


Figure 1. K_s band image of the PSR B1957+20 system. The arrow indicates the position of the secondary with the line of sight contaminator ($0.7''$ separation) lying to the north east. The exposure time was 180s.

which at the time of our observations was accurate to at least 1 second. Our final K_s -band photometry is displayed in Table 1.

Previous attempts at IR photometry of this system were unable to resolve the pulsar from the line of sight contaminator and as such only the K-band magnitude of the unresolved combination was obtained (see Eales et al. 1990). However, our new observations allow us to subtract the magnitude of the contaminator from the combined magnitude of Eales et al. (1990), yielding a K_s -band magnitude of the system at maximum of 17.8 ± 0.1 .

3 THE ELC MODEL

To model these data we used the ELC light curve modelling code (Orosz et al. 2000). The ELC code is ideally suited for this type of system as it incorporates the NEXTGEN low temperature model atmosphere tables, which are critical for systems like PSR B1957+20, with a companion of likely temperature ~ 3000 K (Fruchter et al. 1995). The ELC code also allows one to fit light curves on a one by one or simultaneous basis. In our case this allowed the fitting of the BVRI and K-band light curves simultaneously.

² IRAF is distributed by the National Optical Astronomy Observatories, which are operated by the Association of Universities for Research in Astronomy Inc., under cooperative agreement with the National Science Foundation.

Table 2. Orbital Parameters of PSR B1957+20 system used in the ELC modelling.

Parameter	Value
Companion Mass ¹	0.022 M_{\odot}
Orbital Period ¹	9.17 hr
$\log L_{\text{spindown}}$ ¹	35.20 erg s ⁻¹
Companion Effective Temp ²	2800 K
Inclination ³	50 – 80°
f^3	~ full

¹ Fruchter et al. 1988 ; ² Fruchter et al. 1995

³ Callanan et al. 1995

3.1 The Model

The ELC program requires a number of input parameters before modelling the light curve: the initial parameters used are given in Table 2. The temperature dependent gravity darkening exponents of Claret (2000) were used. We initially attempted to model the system as a blackbody ($T \sim 2800$ K); however, the results were unsatisfactory. While the code had no problem in fitting the observed light curve at maximum, it was completely incapable of reproducing the observed minimum (the model was consistently too luminous during eclipse). We then employed the NEXTGEN model atmospheres of Hauschildt, Allard & Baron (1999a) & Hauschildt et al. (1999b), and using our blackbody model as our starting point, we proceeded to model the light curve. The pulsar mass was set to the canonical value of $1.4 M_{\odot}$. We then varied the following parameters: inclination and mass ratio of the system, Roche lobe filling fraction (f), temperature and bolometric albedo (a) of the secondary star and the irradiating luminosity. The geneticELC algorithm (based on the PIKAIA routine of Charbonneau 1995) was used to search for the best fit values. The best fit R-band model is displayed in Figure 2. We see that there is excellent agreement between the fit and the data ($\chi^2_{\nu} = 1.06$). The largest deviations occur at orbital phases $\phi > 0.65$, but even these are well within the errors. This discrepancy is due to the relative faintness of the companion at these phases, and poorer seeing conditions during these observations. As a check on the validity of the model we used our limited K_s-band data, as displayed in Figure 3. We see that the fit agrees with these data very well.

Given that the mass of the pulsar is currently unknown, although most evolutionary scenarios suggest that it will have accreted a few $1/10^{\text{th}}$ of a solar mass from the secondary, we decided to repeat the above procedure for a number of other primary masses in the range $1.3 < M_{\text{MSP}} < 1.9 M_{\odot}$, to investigate the effect of the pulsar’s mass on our estimates of the mass ratio and orbital inclination of the system.

4 RESULTS

4.1 Inclination

At a given pulsar mass the inclination was constrained to within $\sim \pm 1.2^\circ$, i.e. for a pulsar of mass $1.4 M_{\odot}$, $i = 64.4^{+1.3}_{-1.2}$ (see Figure 4), and overall for the above range of pulsar masses we find the inclination of the system to be in the range, $63^\circ \leq i \leq 67^\circ$, at the 3σ level.

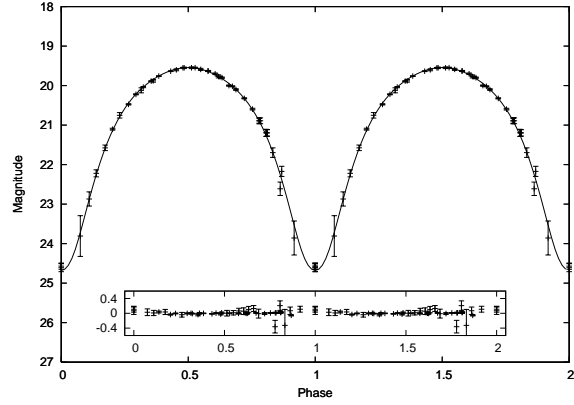


Figure 2. The best fit to the combined R-band data with residuals (inset). Two orbital phases are displayed for added clarity. The pulsar mass is $1.4 M_{\odot}$. The best fit inclination is $i = 64.4^{+1.3}_{-1.2}$ (3σ) with a $\chi^2_{\nu} = 1.06$

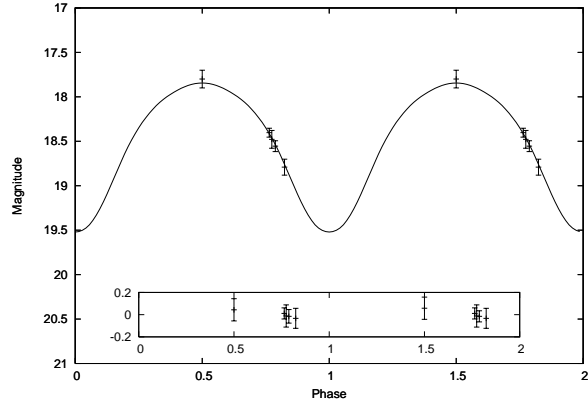


Figure 3. The simultaneous fit to the K-band light curve corresponding to the R-band fit in Figure 2.

4.2 Pulsar Mass

The value of χ^2_{ν} exhibited only a nominal increase as the mass of the pulsar was increased from $1.3 - 1.9 M_{\odot}$; hence our models are unable to constrain this parameter.

4.3 Roche lobe filling factor

At no point in our attempts to model this system were we able to obtain an acceptable fit for a secondary filling its Roche lobe. For our models using the NEXTGEN model atmospheres the value of f was approximately constant, $0.81 \leq f \leq 0.87$ (3σ level), as we varied the mass of the pulsar between 1.3 and $1.9 M_{\odot}$. Hence the secondary is tightly constrained as not currently filling its Roche lobe.

4.4 Temperature of the Secondary at maximum and minimum

We obtained a value of $T = 2900 \pm 110$ K (3σ level), for the effective temperature of the un-illuminated side of the companion star

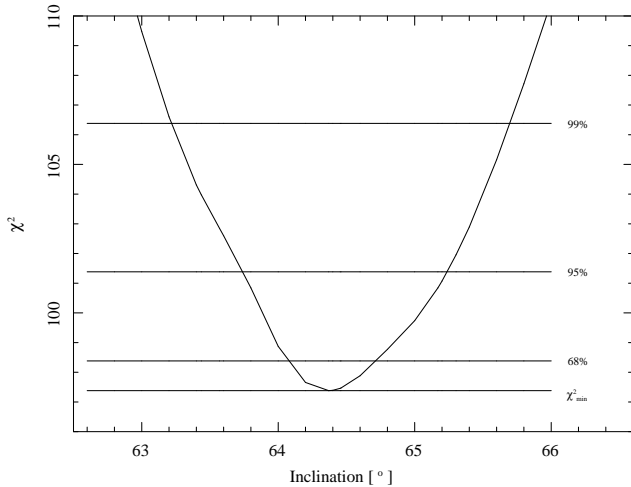


Figure 4. The graph of χ^2 vs i for a pulsar of mass $1.4 M_{\odot}$. Minimum occurs for $\chi^2_{\min} = 96.4$ and an inclination, $i \sim 64.4^\circ$. The 68%, 95% & 99% confidence levels are illustrated.

for pulsar masses in the range $1.3 - 1.9 M_{\odot}$. For individual pulsar masses the 3σ error was ± 90 K i.e. for a pulsar of mass $1.4 M_{\odot}$ an effective temperature of $T = 2900 \pm 90$ K was obtained. The corresponding temperature at maximum is $T = 8300 \pm 200$ K (3σ).

From our modelling, we have obtained the magnitude of the secondary at maximum (in I) and during eclipse (in B, V and K); see Table 3. These provide us with colour information about both the cool side and the irradiated side of the pulsar's companion.

We find that at least $\sim 70\%$ of the spin-down energy of the pulsar is required to produce the observed heating effect and that this percentage is independent of the mass of the pulsar. The bolometric albedo of the system was found to remain close to a value of 0.5 for all our models, which ensured that the secondary was convective.

5 DISCUSSION

We have modelled the light curve of the PSR B1957+20 system with the ELC code and we find the system to be accurately modelled by a highly irradiated secondary. The inclination of the system is measured to be $65^\circ \pm 2^\circ$ for a pulsar in the mass range $1.3 - 1.9 M_{\odot}$.

The optical/IR lightcurves display no evidence for the presence of a contribution from the intra-binary shock. If such a shock did contribute in a non-negligible manner to the optical/IR flux from the system, we would expect to observe this in the form of an asymmetrical distortion of the lightcurves, which is not observed. In contrast the highly symmetrical nature of the lightcurves is striking evidence that the modulation is the result of the emission from the heated face of the secondary star. Bogdanov et al. (2005) observed variable non-thermal X-ray emission attributed to the intra-binary shock in the binary millisecond pulsar 47 Tuc W³; however, an extrapolation of this emission to optical wavelengths demonstrated that it contributed negligibly here. Recent *XMM-Newton* observations (Huang et al. 2007) have tentatively detected similar emission in the PSR B1957+20 system, although our observations

show it to have an insignificant contribution in the optical, as observed in 47 Tuc W.

5.1 The Roche lobe filling factor

The Roche lobe filling factor is constrained to be greater than 80%, for our best fit model. This result is in agreement with past estimates that required the secondary to be close to filling its Roche lobe (Aldcroft et al. 1992; Applegate et al. 1994; Brookshaw et al. 1995; Callanan et al. 1995). Previous estimates of the mass loss rate in this system (Fruchter & Goss 1992) required the system to be close to filling its Roche lobe, as the measured density of the eclipsing material was too tenuous to account for significant mass loss. They claimed that if the secondary neared its Roche lobe, material could easily leave the stellar surface and remain in the orbital plane; this would explain the low density of the observed material.

5.2 Temperature and albedo of the secondary star

The effective temperature of the un-illuminated side of the secondary, $T = 2900 \pm 110$ K, is in excellent agreement with the previous estimate of $T = 2800 \pm 150$ K (Fruchter et al. 1995) and is corroborated by its agreement with the R - I colour temperature obtained via the HST (~ 3000 K, Cox 2000). The temperature derived from the colour information at maximum is $T_{max} = 8000^{+1000}_{-3000}$ K. This compares with a temperature of 8300 ± 200 K from the ELC models. The error in the colour temperature at maximum is dominated by the large uncertainty in the extinction in the direction of PSR B1957+20.

The bolometric albedo of the secondary, defined as the ratio of the reradiated energy to the irradiance energy (Wilson 1990), was found to favour the convective case ($a \sim 0.5$) as one would expect for a secondary of such a small size (King et al. 2005). We note here the modelling of the analogous system PSR J2051-0827 (Stappers et al. 2001), in which the percentage of the pulsar's spin-down luminosity, which is re-radiated in the optical by the secondary, was determined to be in the region of 30% - 45%. This is consistent with the incident spin-down luminosity that our models require for PSR B1957+20 ($\geq 70\%$), given the above albedo.

As a check, a number of models were constructed in which the bolometric albedo was set to 1.0 (radiative secondary). In this case, the best fit value of the irradiating luminosity is found to be lower as expected but the associated temperature of the cool side of the secondary is inconsistent with the observed colours.

5.3 Temperature Gradient

It is clear from the light curve of PSR B1957+20 that a large temperature gradient is required between the heated and cool hemispheres of the companion star. To test if this is physically sustainable, we decided to model the heat flow along the surface of the secondary in more detail.

A two-dimensional model of the irradiation of PSR B1957+20 was simulated using a modified version of the code described in Beer & Podsiadlowski (2002). The code uses a polytropic equation of state and only hydro-dynamical effects were initially considered. The irradiation causes a stress on the stellar surface which drives a sub-sonic circulation. Once this circulation pattern was found thermodynamic effects were considered. Matter in the directly illuminated region was heated and the advection of this mat-

³ also known as PSR J0024-7204

Table 3. Optical and IR magnitudes of the companion to PSR B1957+20 at maximum and during eclipse.

	B	V	R	I	K
Max	21.08 ± 0.05	20.16 ± 0.05	19.53 ± 0.05	18.79 ± 0.05	17.8 ± 0.1
Min	28.1 ± 0.1	26.2 ± 0.1	24.6 ± 0.1	22.52 ± 0.05	19.5 ± 0.1

The values in bold are predicted by the ELC models, all other values are measured directly from the photometry.

ter was followed across the stellar surface. As the matter flowed it was allowed to cool radiatively. The resulting temperature distribution was evolved in time until a steady-state solution was achieved. It was found that the heated material extended beyond the directly irradiated region but that not all of the un-illuminated portion of the star was heated. Consequently a large temperature gradient between the illuminated and un-illuminated sides was found to exist.

It may not be obvious how such a large temperature gradient can exist across the surface of the secondary. In fact the converse has also been argued. If the radiative cooling timescale is short then little or no energy would be redistributed (Dahab 1974). The reason why a large temperature gradient can exist is because the star is perturbed from hydrostatic equilibrium by the irradiation induced circulation as first noted by Kippenhahn & Thomas (1979). The circulation pattern attempts to distribute the energy due to heating across the surface of the secondary. However, the circulation itself, produces inertia terms in the equations of motion which perturb the star from hydrostatic equilibrium i.e. the pressure gradient is no longer in the same direction as the potential gradient. This in turn is what allows the large temperature gradient to exist across the surface, even of a star as small as the secondary present in this system. This effect is independent of whether the object in question is degenerate or non-degenerate.

5.4 Nature of the secondary

We can use the above colour/temperature information to constrain the nature of the secondary star. The colour information appears to rule out the possibility that the secondary is a white dwarf. In their study of ultracool white dwarfs ($T < 4000$ K) Gates et al. (2004) found that white dwarfs at this low temperature typically have $R-I < 0.5$, whereas we find $(R-I)_0 = 1.8 \pm 0.3$. The reddening in the direction of PSR B1957+20 was calculated using the hydrogen column density estimate of Stappers et al. (2003), $N_H = (1.8 \pm 0.7) \times 10^{21} \text{ cm}^{-2}$, in combination with the extinction curve of Savage et al. (1979). Furthermore, if the secondary in PSR B1957+20 was a $\sim 0.025 M_\odot$ white dwarf, one would expect a radius of $\sim 0.1 R_\odot$ - again in contrast with the value of $\sim 0.3 R_\odot$ which we have determined from our modelling.

According to Bessell (1991) $R - I$ is the most reliable spectral type indicator for late M-type stars and using their diagrams of both spectral type & temperature vs $R - I$ for a sample of late M dwarfs, we find that temperatures of between 2900 - 3100 K and spectral types of M4 - M7 are in agreement with our observed $R - I$. Hence the secondary appears to exhibit the colours of a late M-type dwarf, although a main sequence companion ($M_{comp} > 0.08 M_\odot$) is ruled out on the basis of the mass function combined with our inclination estimate above. It is clear that the current mass of the secondary is well below the hydrogen burning limit of $0.08 M_\odot$. Hence, the most likely current state of the secondary is that of a brown dwarf.

The low mass secondary in this system has been observed to have a temperature of ~ 2900 K and a radius encompassing $\sim 80\%$

of its Roche lobe. In contrast a 50 Myr old $0.025 M_\odot$ brown dwarf would be expected to have a temperature of ~ 2200 K and a radius approximately half the size of that observed (Chabrier et al. 2000). Applegate et al. (1994) have previously proposed a model in which the secondary star is heated to this temperature through tidal heating; this model also has the advantage of naturally explaining the orbital period variability observed by Arzoumanian et al. (1994). However, this model requires the secondary star to be close to filling its Roche lobe and given that we observe the secondary to be underfilling its Roche lobe by up to 20%, it is questionable if tidal heating would be an efficient heating mechanism in this scenario.

The accreting millisecond pulsar SAX J1808.4-3658 is also observed to have a bloated, low mass ($\sim 0.05 M_\odot$) companion. In this case Bildsten & Chakrabarty (2001) suggest that the secondary star is 'pumped up' to the bloated higher entropy state by the heating effect of the thermal radiation emitted by the neutron star in quiescence. One could envisage the secondary star in PSR B1957+20 being affected in a similar manner but in this case the heating would be caused by the incident spin-down radiation from the radio pulsar. In reality the situation is likely to be a complicated interplay between both mechanisms which combine to produce the abnormal secondary present in this system.

5.5 Comparison with other MSPs

At this point we should also compare our results with the other ablating field system PSR J2051-0827 (Stappers et al. 1999, 2001), which is remarkably similar to PSR B1957+20. The secondary in this system appears to be similar to that in PSR B1957+20. It has a mass of $\sim 0.025 M_\odot$ and the temperature of the cool side has been measured to be ~ 3000 K. This system has also been found to be under-filling its Roche lobe, in this case by $\sim 50\%$. Even though the orbital period of this system is only 2.4 hrs (in comparison to 9.1 hrs for PSR B1957+20), it is clear that a similar ablation mechanism is at work.

Interest in these ablating systems has increased with the discovery of the accretion powered X-ray millisecond pulsars (AXMPs). There is evidence that the pulsar in these systems is in the process of 'turning-on' as a radio pulsar. In the AXMP SAX J1808.4-3658 (in't Zand et al. 1998), consisting of a neutron star and a secondary of mass $\sim 0.05 M_\odot$ (Bildsten & Chakrabarty 2001), a similar process could be taking place. Once again the secondary is being heated, but in this case the cool side of the secondary is only 1000 K cooler than the warm side. Campana et al. (2004) have interpreted this as evidence that the companion star is being irradiated by the spin down luminosity of the pulsar. Further observations of quiescent AXMPs are required to test this hypothesis (e.g. Callanan et al. 2007).

6 CONCLUSIONS

The main aim of this paper was to constrain the inclination of the system as a precursor to a campaign of phase resolved spectroscopy, with the aim of measuring the mass of the pulsar. We have determined the inclination to within $\pm 2^\circ$ for a pulsar mass in the range $1.3 - 1.9 M_\odot$. This should ensure that any mass determination will be limited only by the accuracy of the radial velocity measurements. We have shown that the temperature of the secondary agrees with previous estimates and the observed temperature gradient is physically sustainable. We also find the secondary to be under-filling its Roche lobe by up to 20%.

We thank Jerome Orosz for kindly providing us with the ELC code.

This paper includes data gathered with the 6.5 meter Magellan Telescopes located at Las Campanas Observatory, Chile. This research has utilized 2MASS data products. The Two Micron All Sky Survey is a joint project of the University of Massachusetts and the Infrared Processing and Analysis Centre/California Institute of Technology, funded by NASA and the National Science Foundation. This research made extensive use of the SIMBAD database, operated at CDS, Strasbourg, France and NASA's Astrophysics Data System.

MTR and PJC acknowledge financial support from Science Foundation Ireland. MAPT was supported in part by NASA LTSA grant NAG5-10889.

REFERENCES

- Aldcroft T.L., Romani R.W., Cordes J.M., 1992, *ApJ*, 400, 638
 Applegate J.H., Shaham J., 1994, *ApJ*, 436, 312
 Arzoumanian Z., Fruchter A.S., Taylor J.H., 1994, *ApJ*, 426, 85
 Backer D., Kulkarni S., Heiles C., Davies M., Goss W.M., 1982, *Nature*, 300, 615
 Beer M.E., Podsiadlowski Ph., 2002, *MNRAS*, 335, 358
 Bessell M.S., 1991, *AJ*, 101, 662
 Bhattacharya D., van den Heuvel E.P.J., 1991, *Phys. Rep.*, 203, 1
 Bildsten L., Chakrabarty D., 2001, *ApJ*, 557, 292
 Bogdanov B., Grindlay J., van den Berg M., 2005, *ApJ*, 630, 1029
 Brookshaw L., Tavani M., 1995, in Fruchter A.S., Tavani M. & Backer D.C., eds, *Millisecond pulsars. A decade of surprise*, ASP Conf Ser, San Francisco
 Callanan P.J., Charles P.A., van Paradijs J., 1989, *MNRAS*, 240, 31
 Callanan P.J., van Paradijs J., Rengelink R., 1995, *ApJ*, 439, 928
 Callanan P.J., Reynolds M.T., Filippenko A.V., Foley R., Garavich P.M., 2007, in prep.
 Campana S., D'Avanzo P., Casares J., Covino S., Israel G., Marconi G., Hynes R., Charles P., Stella L., 2004, *ApJ*, 614, 49
 Chabrier G., Baraffe I., Allard F., Hauschildt P., 2000, *ApJ*, 542, 464
 Charbonneau P., 1995, *ApJS*, 101, 309
 Claret A., 2000, *A&A*, 359, 289
 Cox A.N., 2000, in Cox A.N., ed., *Allen's Astrophysical Quantities*, 4th edn. AIP/Springer-Verlag, New York
 Dahab R.E., 1974, *ApJ*, 187, 351
 Eales S.A., Becklin E.E., Zuckerman B., McLean I.S., 1990, *MNRAS*, 242, 17
 Eichler D., Levinson A., 1988, *ApJ*, 335, L67
 Fruchter A.S., Stinebring D.R., Taylor J.H., 1988, *Nature*, 333, 237
 Fruchter A.S., Goss W.M., 1992, *ApJ*, 384, L47
 Fruchter A.S., Bookbinder J., Bailyn C.D., 1995, *ApJ*, 443, 21
 Gates E., Gyuk G., Harris H.C. et al., 2004, *ApJ*, 612, 129
 Hauschildt P.H., Allard F., Baron E., 1999, *ApJ*, 512, 377
 Hauschildt P.H., Allard F., Ferguson J., Baron E., Alexander D.R., 1999, *ApJ*, 525, 871
 Holtzman J.A., Burrows C.J., Casertano S., Hester J.J., Trauger J.T., Watson A.M., Worthey G., 1995, *PASP*, 107, 1065
 Huang H.H., Becker W., 2007, *A&A*, 463, 5
 in't Zand J.J.M., Heise J., Muller J.M., Bazzano A., Cocchi M., Natalucci L., Ubertini P., 1998, *A&A*, 331, 25
 King A.R., Davies M.B., Beer M.E., 2003, *MNRAS*, 345, 678
 King A.R., Beer M.E., Rolfe D.J., Schenker K., Skipp J.M., 2005, *MNRAS*, 358, 1501
 Kippenhahn R., Thomas H.C., 1979, *A&A*, 75, 281
 Kulkarni S.R., Djorgovski S., Fruchter A.S., 1988, *Nature*, 334, 504
 Levinson A., Eichler D., 1991, *ApJ*, 379, 359
 Leggett S.K., 1992, *ApJS*, 82, 351
 Lorimer D.R., <http://www.livingreviews.org/Articles/Volume4/>
 Manchester R. N., Hobbs G. B., Teoh A., Hobbs, M., 2005, *AJ*, 129, 1993
 Orosz J.A., Hauschildt P.H., 2000, *A&A*, 364, 265.
 Persson S.E., Murphy D.C., Krzeminski W., Roth M., Rieke M.J., 1998, *AJ*, 116, 2475
 Phinney E.S., Kulkarni S.R., 1994, *ARA&A*, 32, 591
 Ruderman M., Shaham J., Tavani M., 1989a, *ApJ*, 336, 507
 Ruderman M., Shaham J., Tavani M., Eichler D., 1989b, *ApJ*, 343, 292
 Ryba M.F., Taylor J.H., 1991, *ApJ*, 380, 557
 Savage B.D., Mathis J.S., *ARA&A*, 17, 73
 Stappers B.W., van Kerkwijk M.H., Lane B., Kulkarni S.R., 1999, *ApJ*, 510, 45L
 Stappers B.W., van Kerkwijk M.H., Bell J.F., Kulkarni S.R., 2001, *ApJ*, 548, 183
 Stappers B.W., Gaensler B.M., Kaspi V.M., van der Klis M., Lewin W.H.G., 2003, *Sci*, 299, 1372
 Stetson P., 1987, *PASP*, 99, 101
 Wilson R.E., 1990, *ApJ*, 356, 613

This paper has been typeset from a \TeX / \LaTeX file prepared by the author.